RMetS

Royal Meteorological Society

New Saharan wind observations reveal substantial biases in analysed dust-generating winds

Alexander J. Roberts,[1]* John H. Marsham,[1] Peter Knippertz,[2] Douglas J. Parker,[1] Mark Bart,[3] Luis Garcia-Carreras,[1] Matthew Hobby,[1] James B. McQuaid,[1] Philip D. Rosenberg[1] and Daniel Walker[4]

[1]*Institute for Climate and Atmospheric Science, School of Earth and Environment, University of Leeds, UK*
[2]*Institute of Meteorology and Climate Research, Karlsruhe Institute of Technology, Germany*
[3]*Air Quality Ltd., Auckland, New Zealand*
[4]*National Centre for Atmospheric Science, University of Leeds, Leeds, UK*

Correspondence to:

*A. J. Roberts, School of Earth and Environment, University of Leeds, LS2 9JT, UK.
E-mail: a.j.roberts1@leeds.ac.uk*

Abstract

For the remote Sahara, the Earth's largest dust source, there has always been a near-absence of data for evaluating models. Here, new observations from the Fennec project are used along with Sahelian data from the African Monsoon Multidisciplinary Analysis (AMMA) to give an unprecedented evaluation of dust-generating winds in the European Centre for Medium-Range Weather Forecasts ERA-Interim reanalysis (ERA-I). Consistent with past studies, near-surface, high-speed winds are lacking in ERA-I and the diurnal variability is under-represented. During the summer monsoon season, correlations of ERA-I with observed wind-speed are low (∼0.35 in Sahel and 0.25–0.4 in the Sahara). Fennec data show for the first time that: (1) correlations are reduced even in the Sahara, not directly influenced by the monsoon, (2) the systematic underestimation of observed winds by ERA-I in the summertime Sahel extends into the central Sahara: potentially explaining the failure of global models to capture the observed global dust maximum that occurs over the summertime Sahara (such as CMIP5), and demonstrates that modelled winds must be improved if they are to capture this key feature of the climatology.

Keywords: fennec; AMMA; dust; reanalysis; monsoon; Sahara;

1. Introduction

The Sahara/Sahel is the world's largest dust source but wind remains a key uncertainty in modelling emission (Knippertz and Todd, 2012). The relative importance of dust raising phenomena and their climatologies are poorly understood (Knippertz and Stuut, 2014). Important processes include the breakdown of the nocturnal low-level jet (NLLJ) and haboobs (Heinold *et al.,* 2013). The NLLJ is often underestimated in models (Fiedler *et al.,* 2013; Largeron *et al.,* 2015) and haboobs are missed by models with parametrized convection (Marsham *et al.,* 2011).

Where observations are sparse, the observational constraint on reanalyses can be insufficient, leading to significant errors (Agustí-Panareda *et al.,* 2010; Garcia-Carreras *et al.,* 2013; Roberts *et al.,* 2015). This becomes something of circular problem, in that for regions with very few observations model developers, and researchers commonly use reanalyses as *de-facto* observations. This can be particularly important when we consider the known limitations of models to capture key dust uplift mechanisms.

Large dust biases exist in climate models, such as their inability to capture the observed Saharan summertime maximum (Heinold *et al.,* 2016; Todd and Cavazos-Guerra, 2016). The severe shortage of data from the region has meant systematic analysis of modelled/analysed dust-generating winds has been very limited. Observations are mostly restricted to the inhabited margins and have systematic sampling biases, especially of the diurnal cycle (Cowie *et al.,* 2014).

Here, we compare low-level winds from the ERA-I reanalysis (Persson and Grazzini, 2007; Dee *et al.,* 2011) with new observations from the Sahara from the Fennec field campaign, and also Sahelian observations from the African Monsoon Multidisciplinary Analysis (AMMA) campaign. The value of ERA-I comparisons lies in its widespread use both operationally and for research. It also shares many features (and therefore process errors) with coarse resolution weather and climate models.

2. Methods

Observations of wind-speed are from stations in the Sahara and Sahel (Figure 1(a)). The Fennec campaign was an international consortium project aimed at improving the understanding of meteorology and climate in the Sahara, specifically with a focus on the lifting of desert dust and with observations from both land-based and aircraft platforms in 2011 and 2012 (Washington *et al.,* 2012). Fennec AWSs were distributed in 2011 and operated into 2013 (Hobby *et al.,*

2013). The AMMA field campaign was an international project with the goal of improving the understanding of the West African Monsoon. Both the meteorological dynamics of the system, and the socio-economic impacts were investigated (Lebel *et al.*, 2010). AMMA provides data from the Atmospheric Radiation Measurement (ARM) Mobile Facilities (AMFs) at Niamey, Niger (2006) and three AMMA-CATCH (Couplage de l'Atmosphère Tropicale et du Cycle Hydrologique) stations: Agoufou (2005–2011), Bamba (2005–2010), and Kobou (2008–2010), all in Mali (Lebel *et al.*, 2010). The AMMA-CATCH observations are of particular use due to the long-term nature of the observations.

To resolve the diurnal cycle, 6-hourly ERA-I reanalyses are augmented with forecasts (giving 3-hourly data). Due to gaps in data reanalysis data has been subsampled to match available observations. Fennec observations are at 2 m, and AMMA data at 3 m, ERA-I 10 m winds from the closest grid-box are adjusted to observation heights using the wind profile power law $u = u_r(z/z_r)^\alpha$. u_r is the observed wind-speed at the reference height (z_r), z is the height to be adjusted to, and α is a stability coefficient (nominally 0.143; Touma, 1977). A range of α values is used to represent uncertainty in the conversion of (higher stability at night; α between 0.1 and 0.4, and lower stability in the day; α between 0.1 and 0.2). This uncertainty encompasses that from using a logarithmic wind profile approach with a range of friction velocities and surface roughness lengths. The choice to use the wind profile power law was a pragmatic one, and was driven by the ability to make some meaningful assumptions about the low-level stability whilst also having no wind profile data and virtually no information about surface characteristics.

This study assumes some parity when comparing time-averaged (1-h) winds at a single point with an instantaneous ERA-I grid-box value (1 h at $1–10\,\mathrm{m\,s^{-1}}$ is $3.6–36\,\mathrm{km}$, comparable with a grid-box). This remains an imperfect comparison but this cannot explain the large differences between ERA-I and observations shown here.

Since dust uplift is a cubic function we study both u and wind-speed cubed (u^3) (Marsham *et al.*, 2013b). For the sake of simplicity, however, we do not apply thresholds. Thresholds vary significantly between regions and seasonally (Cowie *et al.*, 2014) and are unknown for these sites. What thresholds to use with ERA-I is also unclear since ERA-I misses rare high wind-speed events. Introducing a threshold would increase the effect of extreme events, increasing disagreements between ERA-I and observations (Cowie *et al.*, 2015).

3. Results

AMMA and Fennec data are analysed separately since their seasonal cycles are generally different (Appendix S1, Supporting information) with the AMMA stations
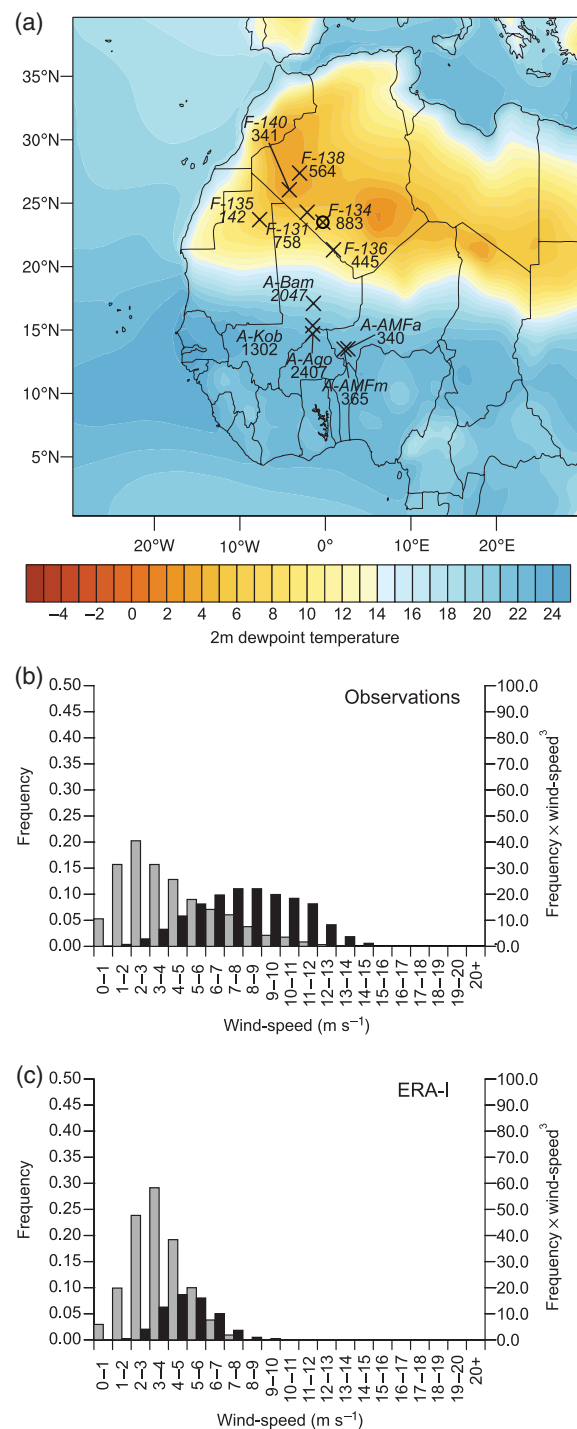
Figure 1. (a) Position of stations, including station identifier and number of days of observations. F, Fennec; A, AMMA. Colour-scale indicates ERA-I 1979–2014 mean August 2 m dewpoint temperature indicating maximum extent of the monsoon. (b) and (c) wind-speed distributions (grey) and distributions multiplied by mean wind-speed cubed (black) for F-134, circled on (a).

being more directly influenced by the West African Monsoon (WAM).

3.1. Wind-speed and wind-power distribution

Figure 1(b) (and Figure 1(c)) show distributions of all observed (ERA-I) u data from the Fennec AWS 134

(F-134). Also shown is the distribution multiplied by the bin mean u^3 giving the wind power. As expected from Cowie *et al.* (2015) and Largeron *et al.* (2015) there is a missing tail of high u events. The area of the wind-power bars (black) should be closely linked with dust uplift (Marsham *et al.*, 2013b). This is much smaller in the ERA-I panel (Figure 1(c)). The peak ERA-I power occurs at $4–5\,ms^{-1}$ (range of $3–8\,ms^{-1}$ across all station grid boxes) compared with $7–8\,ms^{-1}$ in observations ($5–10\,ms^{-1}$ across all stations). In many dust schemes tuning helps to compensate for such issues to match observed dust loads. However, the misrepresentation of rare events and the diurnal cycle remains a problem that tuning cannot overcome. The effect of the scaling uncertainty on the distributions is small, shifting the distribution right slightly for weaker stability and left for stronger stability (not shown). The area of the black bars in the ERA-I plots is always far less than that from observed stations and the ERA-I distributions always are always lacking the high wind-speed tail.

3.1.1. Scatter and best-fit statistics

Figures 2(a) and (b) show scatter graphs for January at a 3-hourly sampling frequency. Figures 2(c) and (d) show the same for daily means. Seasonal variation of best-fit statistics is shown in Figures 2(e) and (f). Rare high wind events are missed in ERA-I, there are no equivalent events missing in observations. This is characteristic of all other months and consistent with ERA-I capturing synoptic-scale features, but missing unresolved uplift processes.

Correlation coefficients for 3-hourly data are lower than those for daily data in both groups (Figures 2(e) and (f)), showing the importance of sub-daily processes on correlation (e.g. NLLJs and haboobs). Correlations for the Fennec (AMMA) group vary seasonally from 0.24 to 0.71 (0.29–0.64) for 3-hourly u, and from 0.22 to 0.68 (0.15–0.65) for 3-hourly u^3 (not shown). Therefore, across both groups ERA-I explains 6–50% of the variance in 3-hourly u and 2–46% of the variance in 3-hourly u^3. A double dip in correlation is present in the AMMA group (Figure 2(e)), temporally coinciding with the passage of the monsoon front. The weakest correlation for the Fennec stations is in August (Figure 2(f)), when the monsoon front is at its most northerly position. Features associated with the edge of the monsoon flow such as strong gradients in humidity and the effects of moist convection are poorly represented in reanalyses (Roberts *et al.*, 2015). The misrepresentation of moist convection during the wet monsoon affects the entire WAM circulation (Garcia-Carreras *et al.*, 2013; Marsham *et al.*, 2013b) leading to lower correlations for Fennec stations beyond the edge of the monsoon flow. Consistent with the low correlations during the monsoon, best-fit line gradients are highest and closest to 1 in winter and lowest (around 0.6) in summer (Figures 2(e) and (f)). Y-intercepts are greater indicating that on average, during the monsoon season ERA-I underestimates (overestimates) light

(strong) winds. However, it is important to note that rare, strong wind-speeds that dominate dust uplift are absent in ERA-I but present in observations.

3.2. Diurnal behaviour

Figure 3 shows that both groups across all months have a too weak diurnal cycle even accounting for stability uncertainty from scaling 10 m winds (dashed red lines). The maximum values (generally during the day), are greatly underestimated in ERA-I. This is particularly pronounced for the Saharan/Fennec stations, consistent with the missing rare winds shown in Figure 1, that contribute disproportionately to u^3.

Night-time ERA-I winds are generally stronger than observed at the Sahel/AMMA stations, consistent with Largeron *et al.* (2015). Possibly caused by artificially enhanced turbulent diffusion in models (Sandu *et al.* 2013) that drives mixing of NLLJ momentum to the surface. At the Fennec stations night-time ERA-I winds are often weaker than observed. This is possibly due to observed winds containing the effects of intermittent shear-driven mixing of momentum to the surface (Schepanski *et al.*, 2015). The shorter inertial oscillation period over the Sahara compared to the Sahel gives greater shear-induced mixing and therefore higher mean surface winds (Heinold *et al.*, 2015). However, differences could also be the result of large-scale pressure gradient errors, which are poorly constrained in reanalyses across the whole region (Roberts and Knippertz, 2014).

The timing of strongest winds in ERA-I is generally correct at the Sahel/AMMA stations but is often too late at the Sahara/Fennec stations. This suggests that modelled NLLJ breakdown takes longer than reality, consistent with inaccurate boundary layer growth (Garcia-Carreras *et al.*, 2015), or enhanced turbulent diffusion artificially raising the height of the NLLJ. The observed 0900 UTC peak in winds (breakdown of the NLLJ) grows in strength in the Sahara/Fennec from March to May and remains strong till October. There is no corresponding increase in u^3 values in ERA-I, again indicating that the winds associated with the NLLJ breakdown are not properly represented in ERA-I in the remote Sahara.

Observed AMMA evening u^3 increases in May, June and July (from approximately 10 to $50\,m^3\,s^{-3}$), this is not present in ERA-I and much less pronounced for the Fennec stations. This suggests that high wind-speeds are missing due to poor representation of convectively generated cold pools (Marsham *et al.*, 2011).

3.3. Seasonal behaviour

Figures 4(a) and (b) show the seasonal development of u^3 for AMMA and Fennec data. Figure 4(c) shows the same for F-136 at Bordj-Badji Mokhtar (BBM). F-136, unlike the other Saharan/Fennec stations, is at the northern limit of haboob uplift in convection-permitting models (Figure 11 in Pantillon *et al.*, 2015) and has been
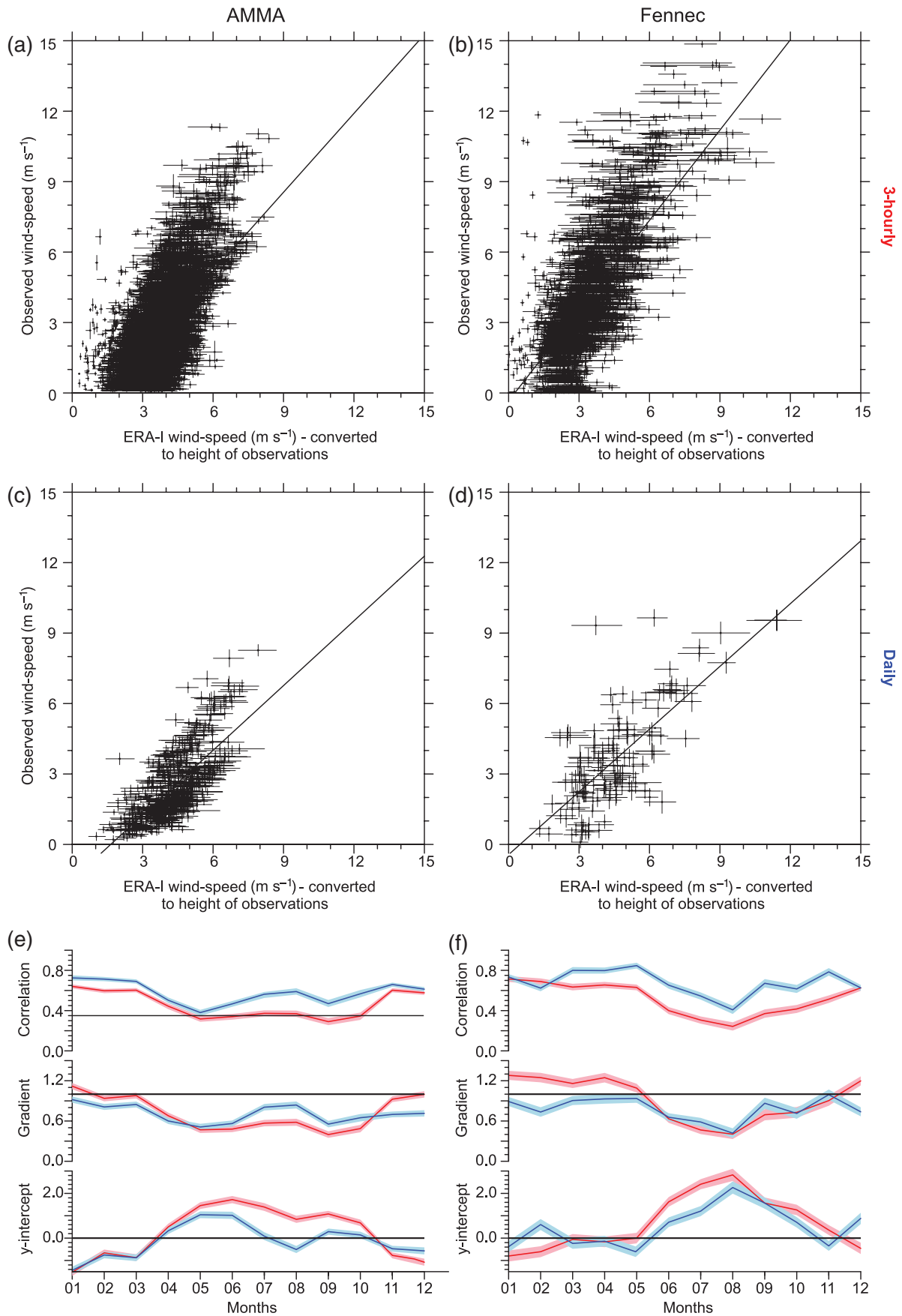
Figure 2. Scatter graphs, AMMA (left) and Fennec (right) for January. (a) and (b) 1-h mean observed against instantaneous ERA-I wind, (3-hourly intervals). (c) and (d) same using daily-mean wind. (e) and (f) seasonal evolution of correlation coefficient and gradient and y-intercept of the best-fit line, 3-hourly (red) and daily (blue). Shading represents ±2 standard deviations of wind uncertainty distribution based on 10 000 iterations of a bootstrapping algorithm.
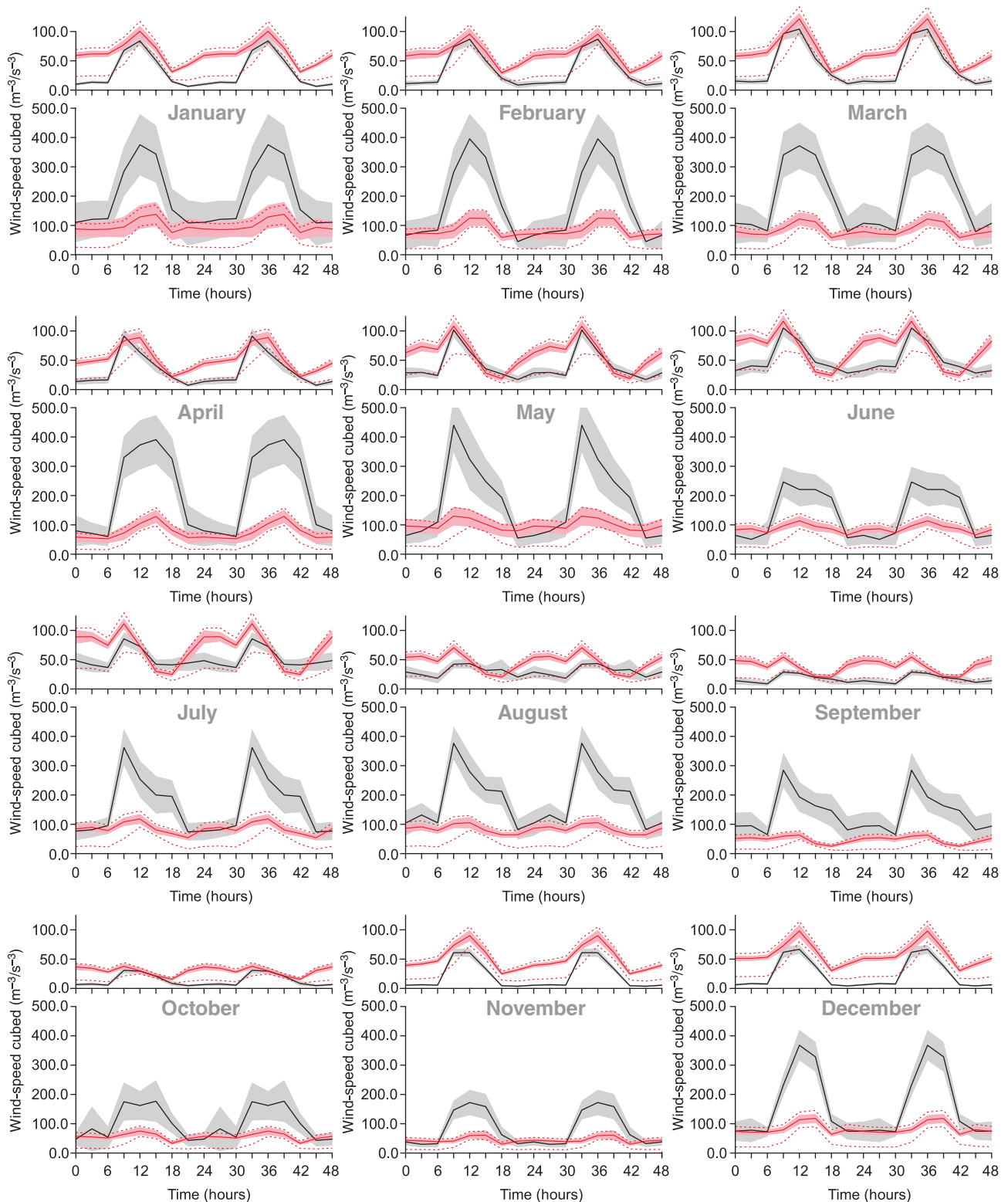
Figure 3. Mean monthly wind-speed cubed diurnal cycle for AMMA (top of panel) and Fennec (bottom), observations (black) and ERA-I (red). Shading represents normalized standard error from monthly diurnal cycle at each station. Dashed red lines indicate the envelope uncertainty associated height conversion of ERA-I winds. Please note the different scales between top and bottom panels.

observed to be regularly affected by moist convection during summer (Marsham *et al.,* 2013a).

ERA-I underestimates the monsoon peak occurring at the AMMA stations (Figure 4(a)), but represents both the variation and magnitude of u^3, during winter.

Observations have greater variability compared to ERA-I at all times of year and increases during the monsoon season for the AMMA stations and at F-136 (Figures 4(a) and (c)). This is consistent with the occurrence of cold pools and their impact on
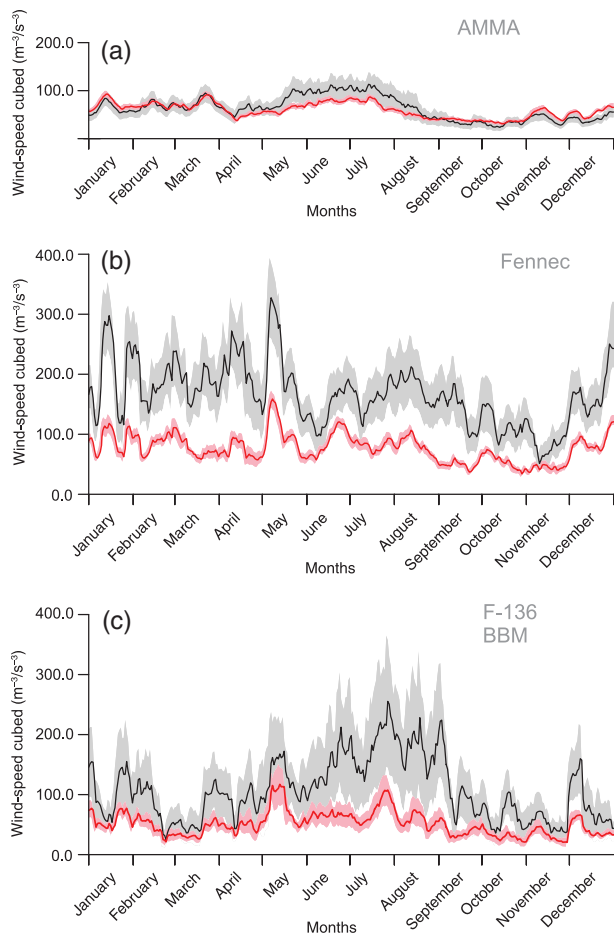
Figure 4. Ten-day running average of daily-mean wind-speed cubed for (a) AMMA, (b) Fennec, and (c) F-136 at BBM showing observations (black) and ERA-I (red). Shading represents normalized standard error of wind-speed cubed from daily-mean for each station.

large-scale meteorology. u^3 values in the Fennec group (Figure 4(b)) are underestimated at all times of year (between 50 and 100 $m^3\,s^{-3}$). Despite this, much of the sub-seasonal variation is captured. ERA-I captures the seasonal and synoptic variability at F-136 in winter, but completely misses the summer maximum which is associated with haboobs (Marsham *et al.,* 2013a).

4. Conclusions

This work gives an unprecedented evaluation of Saharan dust-generating winds from within the summertime dust maximum. We compare new Saharan observations from the Fennec project and Sahelian observations from AMMA with ERA-I reanalysis. These data lack the systematic sampling bias found in routine data from the Sahara (Cowie *et al.,* 2014) and capture a full annual cycle, unlike datasets used previously (Marsham *et al.,* 2013a).

The ERA-I distribution of winds misses rare high wind-speed events. ERA-I's wind-power maxima is $3-8\,ms^{-1}$, compared to $5-10\,ms^{-1}$ in observations. While tuning uplift thresholds can account for

a shortfall in emission, it cannot address important process errors.

For all stations, correlations decrease during the approach of the monsoon front (∼0.8 to ∼0.4), highlighting the poor monsoon representation as a key problem. Three-hourly correlations (0.24–0.71) are worse than those for daily data (0.41–0.84), implicating processes on sub-daily time-scales as being improperly represented by ERA-I (e.g. NLLJs and haboobs).

The diurnal cycle in dust-generating winds is too weak in ERA-I, consistent with artificially high nocturnal mixing in ERA-I. ERA-I also misses stronger day-time winds in the Sahara. The diurnal timing of strongest winds in ERA-I is correct in the Sahel, but too late in the Sahara, likely due to misrepresentation of the NLLJ. There is an increase in afternoon/evening winds in the summer in the Sahel in observations, but not in ERA-I, coinciding with the occurrence haboobs.

In the remote Sahara, ERA-I captures much of the synoptic and seasonal variability and there is no clear summertime maximum in u^3. In the Sahel and southern Sahara the summertime maximum in u^3 is missed by ERA-I.

Climate models fail to capture the central Saharan summertime maxima in dust that is close to BBM (Figure 2 in Todd and Cavazos-Guerra, 2016 and Figures 2 and 6 in Heinold *et al.,* 2016). This key failure of climate models is consistent with the new result shown here that even the observationally constrained ERA-I analyses do not capture the summertime peak in dust-generating winds in the region of the maximum dust loads.

The misrepresentation of uplift processes provides one reason for the lack of reliability of dust in climate models (Evan *et al.,* 2014). It supplies motivation for work focussed on a better understanding of the interactions of multiscale processes within the West African Monsoon, which, due to the inherently complex and chaotic nature of convective systems and the strong horizontal gradients are still not adequately represented in any simulations. Alongside improved representation of the monsoon there is a need for further research into parameterization of haboobs (Pantillon *et al.,* 2016). This work also suggests that caution should be applied when studying dust uplift using analysed winds (Evan *et al.,* 2016). It highlights that climate models (technically similar ERA-I) miss key uplift processes. Therefore, climate predictions of dust are likely to have spatial and temporal errors in uplift, potentially leading to unrealistic dust loadings and transport.

Supporting information

The following supporting information is available:

Appendix S1. Information detailing problems and limitations of observed near surface winds, and seasonal cycles of wind speed cubed plotted for individual observation stations.

References

Agustí-Panareda A, Beljaars A, Cardinali C, Genkova I, Thorncroft C. 2010. Impacts of assimilating AMMA soundings on ECMWF analyses and forecasts. *Weather Forecasting* **25**: 1142–1160.

Cowie SM, Knippertz P, Marsham JM. 2014. A climatology of dust emission events from northern Africa using long-term surface observations. *Atmospheric Chemistry and Physics* **14**: 8579–8597.

Cowie SM, Marsham JH, Knippertz P. 2015. The importance of rare, high-wind events for dust uplift in northern Africa. *Geophysical Research Letters* **42**: 8208–8215.

Dee DP, Uppala SM, Simmons AJ, Berrisford P, Poli P, Kobayashi S, Andrae U, Balmaseda MA, Balsamo G, Bauer P, Bechtold P, Beljaars ACM, van de Berg L, Bidlot J, Bormann N, Delsol C, Dragani R, Fuentes M, Geer AJ, Haimberger HSB, Hersbach H, Hólm EV, Isaksen L, Kållberg P, Köhler M, Matricardi M, McNally AP, Monge-Sanz BM, Morcrette J-J, Park B-K, Peubey C, de Rosnay P, Tavolato C, Thépaut J-N, Vitart F. 2011. The ERA-interim reanalysis: configuration and performance of the data assimilation system. *Quarterly Journal of the Royal Meteorological Society* **137**: 553–597.

Evan AT, Flamant C, Fiedler S, Doherty O. 2014. An analysis of aeolian dust in climate models. *Geophysical Research Letters* **41**: 5996–6001.

Evan AT, Flamant C, Gaetani M, Guichard F. 2016. The past, present and future of African dust. *Nature* **531**: 493–495.

Fiedler S, Schepanski K, Heinold B, Knippertz P, Tegen I. 2013. Climatology of nocturnal low-level jets over North Africa and implications for modeling mineral dust emission. *Journal of Geophysical Research: Atmospheres* **118**: 6100–6121.

Garcia-Carreras L, Marsham JH, Parker DJ, Bain CL, Milton S, Saci A, Salah-Ferroudj M, Ouchene B, Washington R. 2013. The impact of convective cold pool outflows on model biases in the Sahara. *Geophysical Research Letters* **40**: 1647–1652.

Garcia-Carreras L, Parker DJ, Marsham JH, Rosenberg PD, Brooks IM, Lock AP, Marenco F, McQuaid JB, Hobby M. 2015. The turbulent structure and diurnal growth of the Saharan atmospheric boundary layer. *Journal of Atmospheric Science* **72**: 693–713.

Heinold B, Knippertz P, Marsham JH, Fiedler S, Dixon NS, Schepanski K, Laurent B, Tegen I. 2013. The role of deep convection and nocturnal low-level jets for dust emission in summertime West Africa: estimates from convection-permitting simulations. *Journal of Geophysical Research: Atmospheres* **118**: 4385–4400.

Heinold B, Knippertz P, Beare RJ. 2015. Idealized large-eddy simulations of nocturnal low-level jets over subtropical desert regions and implications for dust-generating winds. *Quarterly Journal of the Royal Meteorological Society* **141**: 1740–1752.

Heinold B, Tegen I, Schepanski K, Banks JR. 2016. New developments in the representation of Saharan dust sources in the aerosol-climate model ECHAM6-HAM2. *Geoscientific Model Development* **9**: 765–777.

Hobby M, Gascoyne M, Marsham JH, Bart M, Allen C, Engelstaedter S, Fadel DM, Gandega A, Lane R, McQuaid JB, Ouchene B, Ouladichir A, Parker DJ, Rosenberg PD, Ferroudj MS, Saci A, Seddik F, Todd M, Walker D, Washington R. 2013. The fennec automatic weather station (AWS) network: monitoring the Saharan climate system. *Journal of Atmospheric and Oceanic Technology* **30**: 709–724.

Knippertz P, Todd MC. 2012. Mineral dust aerosols over the Sahara: meteorological controls on emission and transport and implications for modeling. *Reviews of Geophysics* **50**: RG1007. https://doi.org/RG1007.

Knippertz P, Stuut J-B. 2014. Chapter 6. Meteorological aspects of dust storms. In *Mineral Dust: A key Player in the Earth System*. Springer: Dordrecht, Netherlands.

Largeron Y, Guichard F, Bouniol D, Couvreux F, Kergoat L, Marticorena B. 2015. Can we use surface wind fields from meteorological reanalyses for Sahelian dust emission simulations? *Geophysical Research Letters* **42**: 2490–2499.

Lebel T, Parker DJ, Flamant C, Bourlès B, Marticorena B, Mougin E, Peugeot C, Diedhiou A, Haywood JM, Ngamini JB, Polcher J, Redelsperger JL, Thorncroft CD. 2010. The AMMA field campaigns: multiscale and multidisciplinary observations in the west African region. *Quarterly Journal of the Royal Meteorological Society* **136**: 8–33.

Marsham JH, Knippertz P, Dixon NS, Parker DJ, Lister GMS. 2011. The importance of the representation of deep convection for modeled dust-generating winds over West Africa during summer. *Geophysical Research Letters* **38**: L16,803.

Marsham JH, Hobby M, Allen CJT, Banks JR, Bart M, Brooks BJ, Cavazos-Guerra C, Engelstaedter S, Gascoyne M, Lima AR, Martins JV, McQuaid JB, O'Leary A, Ouchene B, Ouladichir A, Parker DJ, Saci A, Salah-Ferroudj M, Todd MC, Washington R. 2013a. Meteorology and dust in the central Sahara: observations from fennec supersite-1 during the June 2011 intensive observation period. *Journal of Geophysical Research: Atmospheres* **118**: 4069–4089.

Marsham JH, Dixon NS, Garcia-Carreras L, Lister GMS, Parker DJ, Knippertz P, Birch CE. 2013b. The role of moist convection in the west African monsoon system: insights from continental-scale convection-permitting simulations. *Geophysical Research Letters* **40**: 1843–1849.

Pantillon F, Knippertz P, Marsham JH, Birch CE. 2015. A parameterization of convective dust storms for models with mass-flux convection schemes. *Journal of Atmospheric Science* **72**: 2545–2561.

Pantillon F, Knippertz P, Marsham JH, Panitz H-J, Bischoff-Gauss I. 2016. Modeling haboob dust storms in large-scale weather and climate models. *Journal of Geophysical Research: Atmospheres* **121**: 2090–2109.

Persson A, Grazzini F. 2007. User Guide to ECMWF forecast products. *Meteorological Bulletin* M3.2 ECMWF

Roberts AJ, Knippertz P. 2014. The formation of a large summertime Saharan dust plume: convective and synoptic-scale analysis. *Journal of Geophysical Research: Atmospheres* **119**: 1766–1785.

Roberts AJ, Marsham JH, Knippertz P. 2015. Disagreements in low-level moisture between (re)analyses over summertime West Africa. *Monthly Weather Review* **143**: 1193–1211.

Sandu I, Beljaars A, Bechtold P, Mauritsen T, Balsamo G. 2013. Why is it so difficult to represent stably stratified conditions in numerical weather prediction (NWP) models? *Journal of Advances in Modeling Earth Systems* **5**: 117–133.

Schepanski K, Knippertz P, Fiedler S, Timouk F, Demarty J. 2015. The sensitivity of nocturnal low-level jets and near-surface winds over the Sahel to model resolution, initial conditions and boundary-layer set-up. *Quarterly Journal of the Royal Meteorological Society* **141**: 1442–1456.

Todd MC, Cavazos-Guerra C. 2016. Dust aerosol emission over the Sahara during summertime from cloud-aerosol lidar with orthogonal polarization (CALIOP) observations. *Atmospheric Environment* **128**: 147–157.

Touma JS. 1977. Dependence of the wind profile power law on stability for various locations. *Journal of the Air Pollution Control Association* **27**: 863–866.

Washington R, Flamant C, Parker DJ, Marsham JH, McQuaid J, Brindley H, Todd MC, Highwood EJ, Chaboureau J-P, Kocha C, Bechir M, Saci A. 2012, 2012. Fennec – the Saharan climate system. *CLIVAR Exchanges* **60**: 31–33.